

Learning-Based Coexistence in Two-Tier Heterogeneous Networks with Cognitive Small Cells

Lin Zhang, *Student Member, IEEE*, Guodong Zhao, *Member, IEEE*, Wenli Zhou, Gang Wu, *Member, IEEE*, Ying-Chang Liang, *Fellow, IEEE*, and Shaoqian Li, *Fellow, IEEE*

Abstract—We study the coexistence problem in a two-tier heterogeneous network (HetNet) with cognitive small cells. In particular, we consider an underlay HetNet, where the cognitive small base station (C-SBS) is allowed to use the frequency bands of the macro cell with an access probability (AP) as long as the C-SBS satisfies a preset interference probability (IP) constraint at macro users (MUs). To enhance the AP (or transmission opportunity) of the C-SBS, we propose a learning-based algorithm for the C-SBS and exploit the distance information between the macro base station (MBS) and MUs. Generally, the signal from the MBS to a specific MU contains the distance information between the MBS to the MU. We enable the C-SBS to analyze the MBS signal on a target frequency band, and learn the distance information between the MBS and the corresponding MU. With the learnt distance information, we calculate the upper bound of the probability that the C-SBS may interfere with the MU, and design an AP with a closed-form expression under the IP constraint. Numerical results indicate that the proposed algorithm outperforms the existing methods up to 60% AP (or transmission opportunity).

Index Terms—Access probability, cognitive small cells, interference probability, learning, underlay HetNet.

I. INTRODUCTION

Recent years have witnessed an explosive growth of the wireless data traffic driven by mobile devices such as smart phones and tablets [1], [2]. To accommodate the tremendous data traffic, mobile operators are pushed to increase the network capacity. However, the existing cellular architecture is designed to provide wide area coverage of users and has limited network capacity. To deal with this issue, the concept of *heterogeneous network* (HetNet) is proposed by embedding the conventional macro cell with multiple small cells [3], [4], [5], [6], [7], [8]. Within a HetNet, a *macro base station* (MBS) is equipped in the macro cell to provide wide area coverage of users. Meanwhile, a *small base station* (SBS) in each small cell is responsible for providing high data rate access for the users within its coverage. Consequently, the HetNet is able to provide both wide area coverage and high network capacity, and is a promising candidate for the next generation of wireless communications.

In the deployment of the HetNet, one of the major challenges is the coexistence issue between small cells and the

macro cell. Among the previous works in [9], [10], [11], [12], [13], [14], there are mainly two categories of coexistence schemes. The first one is overlay HetNet [9], [10], [11], in which frequency resource is divided into two non-overlapped groups. Then, small cells and the macro cell use orthogonal frequency bands to avoid the co-channel interference, but this is inefficient in terms of spectrum efficiency, especially under a sparse small cell deployment. The second one is underlay HetNet [12], [13], [14], in which small cells and the macro cell share the same frequency bands. Then, the underlay HetNet can provide higher spectrum efficiency compared with the overlay HetNet. Nevertheless, a centralized coordinator is expected to manage the co-channel interference between small cells and the macro cell, and raises extra cost.

To deal with the coexistence issue in the HetNet, cognitive techniques are introduced to small cells, namely, cognitive small cells, in which the SBS is equipped with the cognitive capability, namely, cognitive SBS (C-SBS). In particular, the C-SBS is able to learn the status of the frequency bands in the macro cell. Then, the C-SBS can determine whether to access a frequency band or not. There are many contributions on the HetNet with cognitive small cells, e.g., [15], [16], [17], [18], [19], [20], [21]. Specifically, [15], [16], [17] investigated the overlay HetNet and proposed a two-phase opportunistic spectrum access scheme. With this scheme, the C-SBS conducts spectrum sensing on a target frequency band in the first phase. If the frequency band is idle, the C-SBS accesses the frequency band in the second phase. Otherwise, the C-SBS accesses another frequency band or keeps silent. Although the C-SBS and the MBS share the same frequency bands, they use these frequency bands in orthogonal time slots. Then, the co-channel interference from the C-SBS to MUs can be avoided. However, the C-SBS may have rare access opportunities when idle frequency bands are limited, for instance, the traffic load of the macro cell is heavy. [18], [19], [20], [21] investigated the underlay HetNet, where the C-SBS is allowed to share the same frequency bands with the MBS in the same time slots. In particular, [18], [19], [20] adopted the independent stationary point process to model the locations of MUs and designed variable access policies to the busy frequency bands under different criterion, e.g., outage probability, throughput, and spectrum efficiency. [21] developed algorithms to detect whether a specific MU is inside the C-SBS coverage and designed an *access probability* (AP) to the frequency band occupied by the MU under an *interference probability* (IP) constraint.

From [18], [19], [20], [21], we notice that the instantaneous

Lin Zhang, Guodong Zhao, Wenli Zhou, Gang Wu, Ying-Chang Liang, and Shaoqian Li are with the National Key Lab of Science and Technology on Communications, University of Electronic Science and Technology of China, Chengdu, China, emails: linzhang1913@gmail.com, gdngzhao@gmail.com, di_di_zhou@163.com, wugang99@uestc.edu.cn, liangyc@ieee.org, and lsq@uestc.edu.cn; Guodong Zhao is also with Department of Electrical and Computer Engineering, Lehigh University, Bethlehem, PA, USA.

location information of a MU is crucial for the C-SBS to maximize the AP (or transmission opportunity) in the underlay HetNet. In particular, with the instantaneous location information, the C-SBS can access the frequency band when the MU is outside the C-SBS coverage, or the C-SBS can access the frequency band with an AP to satisfy the IP constraint when the MU is inside the C-SBS coverage. On the contrary, without the instantaneous location information, the C-SBS has to consider the worst case and conservatively access the frequency band all the time. This inevitably compromises the AP (or transmission opportunity) of the C-SBS. However, the instantaneous location information of the MU is only available at the MBS and the MU, and is unknown at the C-SBS. Thus, it is challenging for the C-SBS to obtain the instantaneous location information of MUs and maximize the AP (or transmission opportunity).

One straightforward alternative is to utilize the stochastic location information of MUs in [18], [19], [20] and another approach is to utilize partial instantaneous location information of MUs in [21]. However, both schemes provide limited AP (or transmission opportunity) for the C-SBS. In this paper, we propose a learning-based algorithm for the C-SBS and exploit the MBS-MU distance information to enhance the AP (or transmission opportunity). To our best knowledge, this is the first work to enable the C-SBS to learn the MBS-MU distance information and design the AP for the C-SBS to realize the underlay HetNet. To highlight our contributions, we summarize this paper as follows:

- We propose a learning-based method for the C-SBS and exploit the MBS-MU distance information to enhance the AP (transmission opportunity) in the underlay HetNet.
- By enabling the C-SBS to analyze the MBS signal, we learn the MBS-MU distance information, i.e., the relation between the MBS-MU distance and the received *signal-to-noise ratio* (SNR) of the MBS signal at the C-SBS.
- Based on the learnt MBS-MU distance information, we calculate the upper bound of the probability that the C-SBS may interfere with the MU. Then, we design an AP for the C-SBS with a closed-form expression under the IP constraint at the MU.
- We numerically verify that the proposed algorithm outperforms the existing methods up to 60% AP (or transmission opportunity).

The rest of the paper is organized as follows: Section II describes the system model in this paper. Section III develops algorithms for the C-SBS to learn the MBS-MU distance information. In Section IV, we exploit the learnt MBS-MU distance information and design an AP for the C-SBS under the IP constraint. Section V provides numerical results and compares the proposed algorithm with the state of arts. Finally, Section VI concludes the paper.

II. SYSTEM MODEL

We consider a HetNet model in Fig. 1, which consists of a macro cell with radius R and a cognitive small cell with radius r . In particular, MUs are uniformly distributed in the macro cell and the MBS serves each MU with a certain frequency

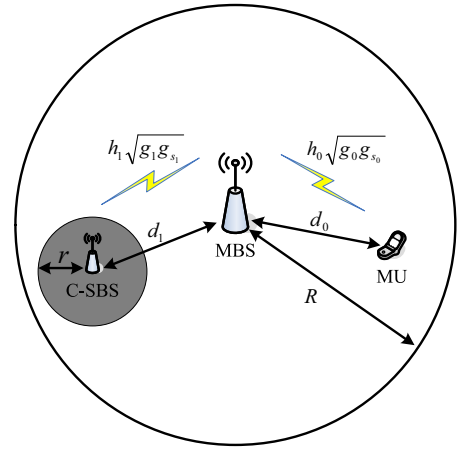


Figure 1. HetNet model, which consists of a macro cell with radius R and a cognitive small cell with radius r . In particular, MUs are uniformly distributed in the macro and the MBS serves each MU with a certain frequency band. Meanwhile, the C-SBS is in the coverage of the MBS and is allowed to access the frequency band being occupied by a MU for coexistence.

band. Meanwhile, the C-SBS is in the coverage of the MBS and is allowed to access the frequency band being occupied by a MU for coexistence. We denote the distance from the MBS to a MU and the C-SBS as d_0 and d_1 , respectively. In what follows, we provide the channel model and the signal model, respectively.

A. Channel Model

We denote h_0 (h_1), g_{s_0} (g_{s_1}), and g_0 (g_1) as the fading, the shadowing, and the path-loss coefficients between the MBS and MU (C-SBS), respectively. Then, the channel between the MBS and the MU (C-SBS) is $h_0 \sqrt{g_0 g_{s_0}}$ ($h_1 \sqrt{g_1 g_{s_1}}$). In particular, $|h_q|$ ($q = 0, 1$) follows a Rayleigh distribution with unit mean. g_{s_q} ($q = 0, 1$) follows a log-normal distribution with standard derivation σ_s . g_q ($q = 0, 1$) is determined by the path-loss model. If we adopt the path-loss model* [22]

$$P_l(d_q) = 128 + 37.6 \log_{10}(d_q), \quad \text{for } d_q \geq \xi, \quad (1)$$

where $\xi = 0.035$ km is the minimum distance between a transmitter and a receiver, g_q can be expressed as

$$g_q = 10^{-12.8} d_q^{-3.76}, \quad \text{for } d_q \geq \xi. \quad (2)$$

For illustrations, we provide the channel model in Fig. 2, where time axis is divided into blocks and each block consists of multiple subblocks. In particular, g_q remains constant all the time for a given d_q , g_{s_q} ($q = 0, 1$) remains constant within each block (i) and varies independently among different blocks, and h_q ($q = 0, 1$) remains constant within each subblock (i, j) and varies among different subblocks.

B. Signal Model

1) *Signal model from the MBS to the MU*: If we denote x_0 as the MBS signal with unit power, i.e., $|x_0|^2 = 1$, and denote

*Although we adopt the path loss model (1) in this paper, our proposed algorithms can be used in other path loss models.

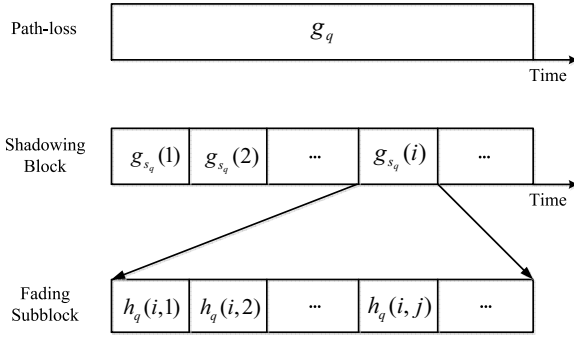


Figure 2. Channel model, where time axis is divided into blocks and each blocks consists of multiple subblocks. In particular, g_q remains constant all the time with a given d_q , g_{s_q} ($q = 0, 1$) remains constant within each block (i) and varies independently among different blocks, and h_q ($q = 0, 1$) remains constant within each subblock (i, j) and varies among different subblocks.

p_0 as the transmit power of the MBS, the received signal at the MU is

$$y_0(i, j) = h_0(i, j) \sqrt{g_0 g_{s_0}(i) p_0(i, j)} x_0(i, j) + n_0(i, j), \quad (3)$$

where (i) denotes the index of the i th block, (i, j) represents the index of the j th subblock in the i th block, n_0 represents the AWGN at the MU with zero mean and variance σ^2 . Then, the SNR of the received signal at the MU is

$$\gamma_0(i, j) = \frac{|h_0(i, j)|^2 g_0 g_{s_0}(i) p_0(i, j)}{\sigma^2}. \quad (4)$$

We further consider that the MBS and the MU adopt *close loop power control* (CLPC) to provide *quality of service* (QoS) guaranteed wireless communication [23], [24]. That is, the MBS automatically adjusts its transmit power to meet a certain target SNR γ_T at the MU. Then, the transmit power of the MBS is

$$p_0(i, j) = \frac{\gamma_T \sigma^2}{|h_0(i, j)|^2 g_0 g_{s_0}(i)}. \quad (5)$$

2) *Signal model from the MBS to the C-SBS*: In the meantime, the received MBS signal at the C-SBS is

$$y_1(i, j) = h_1(i, j) \sqrt{g_1 g_{s_1}(i) p_0(i, j)} x_0(i, j) + n_1(i, j), \quad (6)$$

where n_1 is the AWGN at the C-SBS with zero mean and variance σ^2 . Then, the SNR of the received MBS signal at the C-SBS is

$$\gamma_1(i, j) = \frac{|h_1(i, j)|^2 g_1 g_{s_1}(i) p_0(i, j)}{\sigma^2}. \quad (7)$$

By Substituting (2) and (5) into (7), $\gamma_1(i, j)$ in (7) can be rewritten as

$$\gamma_1(i, j) = \frac{\gamma_T d_1^{-3.76} g_{s_1}(i) |h_1(i, j)|^2}{d_0^{-3.76} g_{s_0}(i) |h_0(i, j)|^2}. \quad (8)$$

III. MBS-MU DISTANCE INFORMATION LEARNING

In this section, we develop an algorithm for the C-SBS to learn the MBS-MU distance information. In principle, when the MBS is transmitting signals to the MU with a target SNR, the transmission is based on the MBS-MU distance. In particular, if the MBS-MU distance is small, the MBS is able to satisfy the target SNR with a small transmit power. This

leads to a small measured SNR at the C-SBS. Otherwise, the MBS has to increase its transmit power to achieve the target SNR. This results in a large measured SNR at the C-SBS. Therefore, the measured SNR at the C-SBS contains the MBS-MU distance information. In what follows, we will first calculate the *cumulative density function* (CDF) of the measured SNR, and then obtain the relation between the MBS-MU distance and the measured SNR.

A. CDF of the SNR at the C-SBS

Removing the time index of the SNR at the C-SBS in (8) and rewriting the SNR in dB, we have

$$\gamma_{1,dB} = \gamma_{T,dB} + 37.6 \log_{10} \left(\frac{d_0}{d_1} \right) + \theta_r + \theta_s, \quad (9)$$

where $\theta_r = 10 \log_{10} (|h_1|^2 / |h_0|^2)$ and $\theta_s = 10 \log_{10} (g_{s_1}) - 10 \log_{10} (g_{s_0})$.

Then, the CDF of $\gamma_{1,dB}$ can be expressed as

$$\begin{aligned} & F_{\Gamma_{1,dB}}(\gamma_{1,dB}) \\ &= \Pr \left\{ \gamma_{T,dB} + 37.6 \log_{10} \left(\frac{d_0}{d_1} \right) + \theta_r + \theta_s \leq \gamma_{1,dB} \right\} \\ &= \Pr \left\{ \theta_r + \theta_s \leq \gamma_{1,dB} - \gamma_{T,dB} - 37.6 \log_{10} \left(\frac{d_0}{d_1} \right) \right\}, \quad (10) \end{aligned}$$

which is related to the distributions of both θ_r and θ_s . In the following, we first calculate the *probability density function* (PDF) of both θ_r and θ_s , and then obtain the CDF of $\gamma_{1,dB}$ with (10).

1) *PDF of θ_r* : Since both $|h_0|$ and $|h_1|$ follow a Rayleigh distribution with unit mean, the CDF of $\phi = |h_1|^2 / |h_0|^2$ is [25]

$$F_{\Phi}(\phi) = \frac{\phi}{1 + \phi}. \quad (11)$$

Then, the CDF of $\theta_r = 10 \log_{10}(\phi)$ is

$$\begin{aligned} F_{\Theta_r}(\theta_r) &= \Pr \{ 10 \log_{10}(\phi) \leq \theta_r \} \\ &= \Pr \left\{ \phi \leq 10^{\frac{\theta_r}{10}} \right\} \\ &= F_{\Phi} \left(10^{\frac{\theta_r}{10}} \right) \\ &= \frac{1}{1 + 10^{-\frac{\theta_r}{10}}}. \quad (12) \end{aligned}$$

Taking the derivation of $F_{\Theta_r}(\theta_r)$, we have the PDF of θ_r as

$$f_{\Theta_r}(\theta_r) = \frac{\ln 10 \cdot 10^{-\frac{\theta_r}{10}}}{10 \left(1 + 10^{-\frac{\theta_r}{10}} \right)^2}. \quad (13)$$

2) *PDF of θ_s* : Recall that both g_{s_0} and g_{s_1} follow a normal distribution with standard derivation σ_s . Then, it is straightforward to obtain that θ_s follows a normal distribution with zero means and variance $2\sigma_s^2$. Thus, the PDF of θ_s is

$$f_{\Theta_s}(\theta_s) = \frac{1}{\sqrt{4\pi\sigma_s^2}} e^{-\frac{\theta_s^2}{4\sigma_s^2}}. \quad (14)$$

Based on (13) and (14), the CDF of $\gamma_{1,dB}$ in (10) can be

calculated as

$$\begin{aligned}
F_{\Gamma_{1,dB}}(\gamma_{1,dB}) &= \Pr\{\theta_r + \theta_s \leq m(\gamma_{1,dB})\} \\
&= \int_{-\infty}^{\infty} \int_{-\infty}^{m(\gamma_{1,dB}) - \theta_s} f_{\Theta_s}(\theta_s) f_{\Theta_r}(\theta_r) d\theta_r d\theta_s \\
&= \int_{-\infty}^{\infty} f_{\Theta_s}(\theta_s) F_{\Theta_r}(m(\gamma_{1,dB}) - \theta_s) d\theta_s, \quad (15)
\end{aligned}$$

where $m(\gamma_{1,dB}) = \gamma_{1,dB} - \gamma_{T,dB} - 37.6 \log_{10} \left(\frac{d_0}{d_1} \right)$.

B. Relation between d_0 and $\gamma_{1,dB}$

To begin with, we provide the following definition.

Definition 1: For a random variable X with CDF $F_X(x)$, $x \in \mathbb{R}$, if $x_{\frac{1}{2}}$ satisfies both $F_X(x_{\frac{1}{2}}) = \Pr\{X \leq x_{\frac{1}{2}}\} = \frac{1}{2}$ and $1 - F_X(x_{\frac{1}{2}}) = \Pr\{X \geq x_{\frac{1}{2}}\} = \frac{1}{2}$, $x_{\frac{1}{2}}$ is defined as the median of the random variable X .

If we denote the median of the random variable $\gamma_{1,dB}$ as $\gamma_{1,dB,\frac{1}{2}}$, we have the following lemma.

Lemma 1: The median of the random variable $\gamma_{1,dB}$ is $\gamma_{1,dB,\frac{1}{2}} = \gamma_{T,dB} + 37.6 \log_{10} \left(\frac{d_0}{d_1} \right)$.

Proof: The detailed proof of this Lemma is provided in Appendix A. ■

From Definition 1 and Lemma 1, the probability that each sample of $\gamma_{1,dB}$ is smaller or larger than $\gamma_{1,dB,\frac{1}{2}}$ is equal to $\frac{1}{2}$. Suppose that the C-SBS observes MBS signals in I blocks and measures $\gamma_{1,dB}$ of J subblocks within each block. Then, the C-SBS can obtain $K = IJ$ independent samples of $\gamma_{1,dB}$, namely, $\gamma_{1,dB}(i, j)$ ($1 \leq i \leq I, 1 \leq j \leq J$). By resorting these K samples in an ascending order, we relabel these samples as $\bar{\gamma}_{1,dB}(k)$ ($1 \leq k \leq K$). Then, we have the relation between the MBS-MU distance and the received SNR $\gamma_{1,dB}$ (or $\bar{\gamma}_{1,dB}$) at the C-SBS in the following Theorem.

Theorem 1: Define a function $f(x) = d_1 10^{\frac{x - \gamma_{T,dB}}{37.6}}$. Then, for a given distance d_0^e from the MBS, the probability that the distance d_0 is larger than d_0^e follows:

- If $d_0^e < f(\bar{\gamma}_{1,dB}(1))$, we have

$$1 - (1/2)^K < \Pr\{d_0^e < d_0\} < 1. \quad (16)$$

- If $d_0^e \geq f(\bar{\gamma}_{1,dB}(K))$, we have

$$0 < \Pr\{d_0^e \leq d_0\} < \left(\frac{1}{2}\right)^K. \quad (17)$$

- If $f(\bar{\gamma}_{1,dB}(k')) \leq d_0^e < f(\bar{\gamma}_{1,dB}(k'+1))$, where $1 \leq k' \leq K-1$, we have

$$\begin{aligned}
&\left(\frac{1}{2}\right)^K (C_K^{k'+1} + C_K^{k'+2} + \dots + C_K^K) \leq \Pr\{d_0^e \leq d_0\} \\
&\leq \left(\frac{1}{2}\right)^K (C_K^{k'} + C_K^{k'+1} + \dots + C_K^K). \quad (18)
\end{aligned}$$

Proof: The detailed proof of this Theorem is provided in Appendix B. ■

Theorem 1 provides both the upper bound and the lower bound of the probability that the MBS-MU distance is in a certain region. With this theorem, we will design the AP of the C-SBS and satisfy the IP constraint at the MU in the next section.

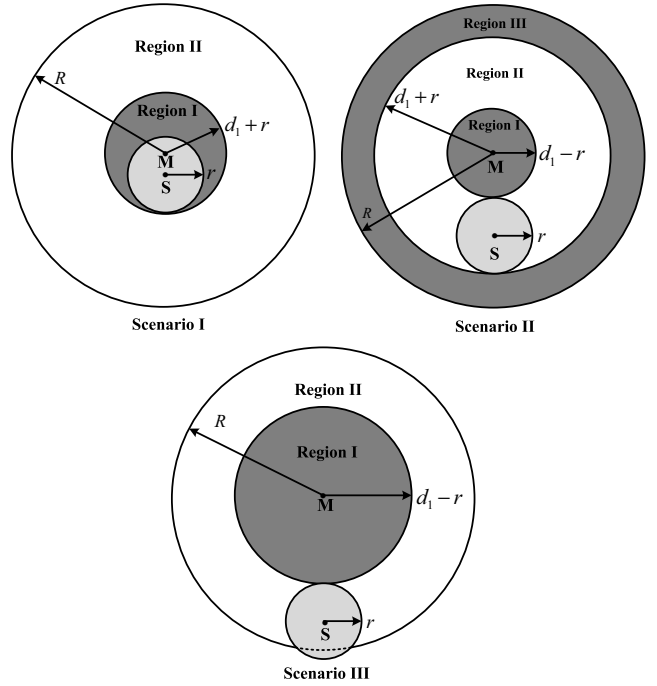


Figure 3. Illustrations of three scenarios, in which the C-SBS is in different locations within the macro cell.

IV. COEXISTENCE BETWEEN THE COGNITIVE SMALL CELL AND THE MACRO CELL

In this section, we utilize the learnt MBS-MU distance information, i.e., relation between d_0 and $\bar{\gamma}_{1,dB}$, to design the AP for the coexistence between the cognitive small cell and the macro cell. We notice that the AP design may be different for distinct locations of the C-SBS within the macro cell. Thus, we will first classify the locations of the C-SBS into three scenarios. Then, we design the AP of the C-SBS in each scenario.

A. Classification of Distinct Scenarios

Based on the MBS-C-SBS distance d_1 , we consider three scenarios as shown in Fig. 3, where points “M” and “S” denote the MBS and the C-SBS, respectively.

- In Scenario I, the MBS-C-SBS distance d_1 is small, i.e., $\xi \leq d_1 \leq r + \xi$. Then, we divide the macro cell into two non-overlapped regions[†], i.e., Region I and Region II. In particular, Region I denotes the region where the distance from the MBS is between ξ and $d_1 + r$, and Region II denotes the region where the distance from the MBS is between $d_1 + r$ and R .

- In Scenario II, the MBS-C-SBS distance d_1 is medium, i.e., $r + \xi < d_1 < R - r$. Then, we divide the macro cell into three non-overlapped regions, i.e., Region I, Region II, and Region III. In particular, Region I denotes the region where the distance from the MBS is between ξ and $d_1 - r$, and Region II denotes the region where the distance from the MBS is between $d_1 - r$ and $d_1 + r$, and Region III denotes the region where the distance from the MBS is between $d_1 + r$ and R .

[†] Since the minimum distance between a transmitter and a receiver is $\xi > 0$, we only consider the regions satisfying the minimum distance.

• In Scenario III, the MBS-C-SBS distance d_1 is large, i.e., $R - r \leq d_1 \leq R + r$. Then, we divide the macro cell into two non-overlapped regions, i.e., Region I and Region II. In particular, Region I denotes the region where the distance from the MBS is between ξ and $d_1 - r$, and Region II denotes the region where the distance from the MBS is between $d_1 - r$ and R .

B. AP Design in Scenario I

In this part, we exploit the results in Theorem 1 to design the AP of the C-SBS and satisfy the IP constraint at the MU in Scenario I, where the macro cell is divided into two regions. In this scenario, the C-SBS may cause interference to the MU if the MU is located in Region I, i.e., $\xi \leq d_0 \leq d_1 + r$. According to the relation between the measured SNRs at the C-SBS and ξ , ξ may satisfy

$$0 < \xi < f(\bar{\gamma}_{1,dB}(1)), \quad (19)$$

or

$$f(\bar{\gamma}_{1,dB}(k_0)) \leq \xi < f(\bar{\gamma}_{1,dB}(k_0 + 1)), \quad (20)$$

for $1 \leq k_0 \leq K - 1$, or

$$f(\bar{\gamma}_{1,dB}(K)) \leq \xi. \quad (21)$$

Meanwhile, according to the relation between the measured SNRs at the C-SBS and $d_1 + r$, $d_1 + r$ may satisfy

$$0 < d_1 + r < f(\bar{\gamma}_{1,dB}(1)), \quad (22)$$

or

$$f(\bar{\gamma}_{1,dB}(k_2)) \leq d_1 + r < f(\bar{\gamma}_{1,dB}(k_2 + 1)), \quad (23)$$

for $1 \leq k_2 \leq K - 1$, or

$$f(\bar{\gamma}_{1,dB}(K)) \leq d_1 + r. \quad (24)$$

Due to the increasing monotonicity of $f(x)$ and $\xi < d_1 + r$, we have six cases of ξ and $d_1 + r$: Case I): ξ satisfies (19) and $d_1 + r$ satisfies (22); Case II): ξ satisfies (19) and $d_1 + r$ satisfies (23); Case III): ξ satisfies (19) and $d_1 + r$ satisfies (24); Case IV) ξ satisfies (20) and $d_1 + r$ satisfies (23); Case V) ξ satisfies (20) and $d_1 + r$ satisfies (24); Case VI) ξ satisfies (21) and $d_1 + r$ satisfies (24).

Next, we first calculate the probability ρ_I that the MU is in Region I for each case and then design the corresponding AP. In the sequential, we denote $S_I = \pi(d_1 + r)^2 - \pi\xi^2$ as the area of Region I, and denote S_c as the area of the interference region, where the MU may appear in the C-SBS coverage. From Appendix C, we have

$$S_c = \begin{cases} \pi r^2 - \pi \xi^2, & \xi \leq d_1 < r - \xi, \\ (\pi - \varphi_2)r^2 - \varphi_1 \xi^2 + d_1 \xi \sin \varphi_1, & r - \xi \leq d_1 \leq r + \xi, \end{cases} \quad (25)$$

where $\varphi_1 = \arccos \frac{d_1^2 + \xi^2 - r^2}{2d_1\xi}$, $\varphi_2 = \arccos \frac{d_1^2 + r^2 - \xi^2}{2d_1r}$.

1) *AP Design in Case I:* In this case, ξ satisfies (19) and $d_1 + r$ satisfies (22). The probability ρ_I that the MU is in

Region I is

$$\begin{aligned} \rho_I &= \Pr \{ \xi \leq d_0 \leq d_1 + r \} \\ &= \Pr \{ d_0 \geq \xi \} - \Pr \{ d_0 \geq d_1 + r \} \\ &\stackrel{(I-a)}{\leq} 1 - 1 + \left(\frac{1}{2}\right)^K \\ &= \left(\frac{1}{2}\right)^K, \end{aligned} \quad (26)$$

where we use (16) in (I-a).

To control the IP constraint η at the MU, the AP of the C-SBS needs to satisfy $0 \leq \rho_{AP} \leq 1$ and $\rho_{AP} \rho_I \frac{S_c}{S_I} \leq \eta$, i.e., $\rho_{AP} \leq \min \left\{ \frac{\eta S_I}{\rho_I S_c}, 1 \right\} = \min \left\{ \frac{\eta [\pi(d_1 + r)^2 - \pi\xi^2]}{\rho_I S_c}, 1 \right\}$, which can be lower bounded by

$$\begin{aligned} &\min \left\{ \frac{\eta [\pi(d_1 + r)^2 - \pi\xi^2]}{\rho_I S_c}, 1 \right\} \\ &\stackrel{(I-b)}{\geq} \min \left\{ \frac{\eta 2^K [\pi(d_1 + r)^2 - \pi\xi^2]}{S_c}, 1 \right\}, \end{aligned} \quad (27)$$

where we use (26) in (I-b).

Thus, to protect the MU in this case, the maximum AP of the C-SBS is

$$\rho_{AP} = \min \left\{ \frac{\eta 2^K [\pi(d_1 + r)^2 - \pi\xi^2]}{S_c}, 1 \right\}, \quad (28)$$

where S_c is shown in (25).

2) *AP Design in Case II:* In this case, ξ satisfies (19) and $d_1 + r$ satisfies (23). The probability ρ_I that the MU is in Region I is

$$\begin{aligned} \rho_I &= \Pr \{ d_0 \geq \xi \} - \Pr \{ d_0 \geq d_1 + r \} \\ &\stackrel{(I-c)}{\leq} 1 - \left(\frac{1}{2}\right)^K \left(C_K^{k_2+1} + C_K^{k_2+2} + \dots + C_K^K \right) \\ &= \left(\frac{1}{2}\right)^K \left(C_K^0 + C_K^1 + \dots + C_K^{k_2} \right), \end{aligned} \quad (29)$$

where we use (16) and (18) in (I-c).

To control the IP constraint η at the MU, the AP of the C-SBS needs to satisfy $0 \leq \rho_{AP} \leq 1$ and $\rho_{AP} \rho_I \frac{S_c}{S_I} \leq \eta$, i.e., $\rho_{AP} \leq \min \left\{ \frac{\eta S_I}{\rho_I S_c}, 1 \right\} = \min \left\{ \frac{\eta [\pi(d_1 + r)^2 - \pi\xi^2]}{\rho_I S_c}, 1 \right\}$, which can be lower bounded by

$$\begin{aligned} &\min \left\{ \frac{\eta [\pi(d_1 + r)^2 - \pi\xi^2]}{\rho_I S_c}, 1 \right\} \\ &\stackrel{(I-d)}{\geq} \min \left\{ \frac{\eta 2^K [\pi(d_1 + r)^2 - \pi\xi^2]}{(C_K^0 + C_K^1 + \dots + C_K^{k_2}) S_c}, 1 \right\}, \end{aligned} \quad (30)$$

where we use (29) in (I-d).

Thus, to protect the MU in this case, the maximum AP of the C-SBS is

$$\rho_{AP} = \min \left\{ \frac{\eta 2^K [\pi(d_1 + r)^2 - \pi\xi^2]}{(C_K^0 + C_K^1 + \dots + C_K^{k_2}) S_c}, 1 \right\}, \quad (31)$$

where S_c is shown in (25).

3) *AP Design in Case III:* In this case, ξ satisfies (19) and $d_1 + r$ satisfies (24). The probability ρ_I that the MU is in

Region II is

$$\rho_I = \Pr \{d_0 \geq \xi\} - \Pr \{d_0 \geq d_1 + r\} \stackrel{(I-e)}{\leq} 1, \quad (32)$$

where we use (16) and (17) in (I-e).

To control the IP constraint η at the MU, the AP of the C-SBS needs to satisfy $0 \leq \rho_{AP} \leq 1$ and $\rho_{AP} \rho_I \frac{S_c}{S_1} \leq \eta$, i.e., $\rho_{AP} \leq \min \left\{ \frac{\eta S_1}{\rho_I S_c}, 1 \right\} = \min \left\{ \frac{\eta[\pi(d_1+r)^2 - \pi\xi^2]}{\rho_I S_c}, 1 \right\}$, which can be lower bounded by

$$\begin{aligned} & \min \left\{ \frac{\eta[\pi(d_1+r)^2 - \pi\xi^2]}{\rho_I S_c}, 1 \right\} \\ & \stackrel{(I-f)}{\geq} \min \left\{ \frac{\eta[\pi(d_1+r)^2 - \pi\xi^2]}{S_c}, 1 \right\}, \end{aligned} \quad (33)$$

where we use (32) in (I-f).

Thus, to protect the MU in this case, the maximum AP of the C-SBS is

$$\rho_{AP} = \min \left\{ \frac{\eta[\pi(d_1+r)^2 - \pi\xi^2]}{S_c}, 1 \right\}, \quad (34)$$

where S_c is shown in (25).

4) *AP Design in Case IV*: In this case, ξ satisfies (20) and $d_1 + r$ satisfies (23). The probability ρ_I that the MU is in Region II is

$$\begin{aligned} \rho_I &= \Pr \{d_0 \geq \xi\} - \Pr \{d_0 \geq d_1 + r\} \\ & \stackrel{(I-g)}{\leq} \left(\frac{1}{2}\right)^K (C_K^{k_0} + C_K^{k_0+1} + \dots + C_K^K) \\ & \quad - \left(\frac{1}{2}\right)^K (C_K^{k_2+1} + C_K^{k_2+2} + \dots + C_K^K) \\ & = \left(\frac{1}{2}\right)^K (C_K^{k_0} + C_K^{k_0+1} + \dots + C_K^{k_2}), \end{aligned} \quad (35)$$

where we use (18) in (I-g).

To control the IP constraint η at the MU, the AP of the C-SBS needs to satisfy $0 \leq \rho_{AP} \leq 1$ and $\rho_{AP} \rho_I \frac{S_c}{S_1} \leq \eta$, i.e., $\rho_{AP} \leq \min \left\{ \frac{\eta S_1}{\rho_I S_c}, 1 \right\} = \min \left\{ \frac{\eta[\pi(d_1+r)^2 - \pi\xi^2]}{\rho_I S_c}, 1 \right\}$, which can be lower bounded by

$$\begin{aligned} & \min \left\{ \frac{\eta[\pi(d_1+r)^2 - \pi\xi^2]}{\rho_I S_c}, 1 \right\} \\ & \stackrel{(I-h)}{\geq} \min \left\{ \frac{\eta 2^K [\pi(d_1+r)^2 - \pi\xi^2]}{(C_K^{k_0} + C_K^{k_0+1} + \dots + C_K^{k_2}) S_c}, 1 \right\}, \end{aligned} \quad (36)$$

where we use (35) in (I-h).

Thus, to protect the MU in this case, the maximum AP of the C-SBS is

$$\rho_{AP} = \min \left\{ \frac{\eta 2^K [\pi(d_1+r)^2 - \pi\xi^2]}{(C_K^{k_0} + C_K^{k_0+1} + \dots + C_K^{k_2}) S_c}, 1 \right\}, \quad (37)$$

where S_c is shown in (25).

5) *AP Design in Case V*: In this case, ξ satisfies (20) and $d_1 + r$ satisfies (24). The probability ρ_I that the MU is in Region I is

$$\begin{aligned} \rho_I &= \Pr \{d_0 \geq \xi\} - \Pr \{d_0 \geq d_1 + r\} \\ & \stackrel{(I-i)}{\leq} \left(\frac{1}{2}\right)^K (C_K^{k_0} + C_K^{k_0+1} + \dots + C_K^K), \end{aligned} \quad (38)$$

where we use (17) and (18) in (I-i).

To control the IP constraint η at the MU, the AP of the C-SBS needs to satisfy $0 \leq \rho_{AP} \leq 1$ and $\rho_{AP} \rho_I \frac{S_c}{S_1} \leq \eta$, i.e., $\rho_{AP} \leq \min \left\{ \frac{\eta S_1}{\rho_I S_c}, 1 \right\} = \min \left\{ \frac{\eta[\pi(d_1+r)^2 - \pi\xi^2]}{\rho_I S_c}, 1 \right\}$, which can be lower bounded by

$$\begin{aligned} & \min \left\{ \frac{\eta[\pi(d_1+r)^2 - \pi\xi^2]}{\rho_I S_c}, 1 \right\} \\ & \stackrel{(I-j)}{\geq} \min \left\{ \frac{\eta[\pi(d_1+r)^2 - \pi\xi^2]}{(C_K^{k_0} + C_K^{k_0+1} + \dots + C_K^K) S_c}, 1 \right\}, \end{aligned} \quad (39)$$

where we use (38) in (I-j).

Thus, to protect the MU in this case, the maximum AP of the C-SBS is

$$\rho_{AP} = \min \left\{ \frac{\eta[\pi(d_1+r)^2 - \pi\xi^2]}{(C_K^{k_0} + C_K^{k_0+1} + \dots + C_K^K) S_c}, 1 \right\}, \quad (40)$$

where S_c is shown in (25).

6) *AP Design in Case VI*: In this case, ξ satisfies (21) and $d_1 + r$ satisfies (24). The probability ρ_I that the MU is in Region I is

$$\rho_I = \Pr \{d_0 \geq \xi\} - \Pr \{d_0 \geq d_1 + r\} \stackrel{(I-k)}{\leq} \left(\frac{1}{2}\right)^K, \quad (41)$$

where we use (17) in (I-k).

To control the IP constraint η at the MU, the AP of the C-SBS needs to satisfy $0 \leq \rho_{AP} \leq 1$ and $\rho_{AP} \rho_I \frac{S_c}{S_1} \leq \eta$, i.e., $\rho_{AP} \leq \min \left\{ \frac{\eta S_1}{\rho_I S_c}, 1 \right\} = \min \left\{ \frac{\eta[\pi(d_1+r)^2 - \pi\xi^2]}{\rho_I S_c}, 1 \right\}$, which can be lower bounded by

$$\begin{aligned} & \min \left\{ \frac{\eta[\pi(d_1+r)^2 - \pi\xi^2]}{\rho_I S_c}, 1 \right\} \\ & \stackrel{(I-l)}{\geq} \min \left\{ \frac{\eta 2^K [\pi(d_1+r)^2 - \pi\xi^2]}{S_c}, 1 \right\}, \end{aligned} \quad (42)$$

where we use (41) in (I-l).

Thus, to protect the MU in this case, the maximum AP of the C-SBS is

$$\rho_{AP} = \min \left\{ \frac{\eta 2^K [\pi(d_1+r)^2 - \pi\xi^2]}{S_c}, 1 \right\}, \quad (43)$$

where S_c is shown in (25).

C. AP design in Scenario II

In this part, we exploit the results in Theorem 1 to design the AP of the C-SBS to satisfy the IP constraint at the MU in Scenario II, where the macro cell is divided into three regions. In this scenario, the C-SBS may cause interference to the MU if the MU is located in Region II, i.e., $d_1 - r \leq d_0 \leq d_1 + r$. According to relation between the measured SNRs at the C-SBS and $d_1 - r$, $d_1 - r$ may satisfy

$$0 < d_1 - r < f(\bar{\gamma}_{1,dB}(1)), \quad (44)$$

or

$$f(\bar{\gamma}_{1,dB}(k_1)) \leq d_1 - r < f(\bar{\gamma}_{1,dB}(k_1 + 1)), \quad (45)$$

for $1 \leq k_1 \leq K - 1$, or

$$f(\bar{\gamma}_{1,dB}(K)) \leq d_1 - r. \quad (46)$$

Meanwhile, according to the relation between the measured SNRs at the C-SBS and $d_1 + r$, $d_1 + r$ may satisfy (22), or (23), or (24).

Due to the increasing monotonicity of $f(x)$ and $\xi < d_1 + r$, we have six cases of $d_1 - r$ and $d_1 + r$: Case I): $d_1 - r$ satisfies (44) and $d_1 + r$ satisfies (22); Case II): $d_1 - r$ satisfies (44) and $d_1 + r$ satisfies (23); Case III): $d_1 - r$ satisfies (44) and $d_1 + r$ satisfies (24); Case IV) $d_1 - r$ satisfies (45) and $d_1 + r$ satisfies (23); Case V) $d_1 - r$ satisfies (45) and $d_1 + r$ satisfies (24); Case VI) $d_1 - r$ satisfies (46) and $d_1 + r$ satisfies (24). Since these six cases in Scenario II are similar to those in Scenario I, we analyze each case and design the corresponding AP in Appendix D.

D. AP Design in Scenario III

In this part, we exploit the results in Theorem 1 to design the AP of the C-SBS to satisfy the IP constraint at the MU in Scenario III, where the macro cell is divided into two regions. In this scenario, the C-SBS may cause interference to the MU if the MU is located in Region II, i.e., $d_1 - r \leq d_0 \leq R$. According to relation between the measured SNRs at the C-SBS and $d_1 - r$, $d_1 - r$ may satisfy (44), or (45), or (46).

Meanwhile, according to the relation between the measured SNRs at the C-SBS and R , R may satisfy

$$0 < R < f(\bar{\gamma}_{1,dB}(1)), \quad (47)$$

or

$$f(\bar{\gamma}_{1,dB}(k_1)) \leq R < f(\bar{\gamma}_{1,dB}(k_1 + 1)), \quad (48)$$

for $1 \leq k_3 \leq K - 1$, or

$$f(\bar{\gamma}_{1,dB}(K)) \leq R. \quad (49)$$

Due to the increasing monotonicity of $f(x)$ and $d_1 - r < R$, we have six cases of $d_1 - r$ and R : Case I): $d_1 - r$ satisfies (44) and R satisfies (47); Case II): $d_1 - r$ satisfies (44) and R satisfies (48); Case III): $d_1 - r$ satisfies (44) and R satisfies (49); Case IV) $d_1 - r$ satisfies (45) and R satisfies (48); Case V) $d_1 - r$ satisfies (45) and R satisfies (49); Case VI) $d_1 - r$ satisfies (46) and R satisfies (49). Since these six cases in Scenario III are similar to those in Scenario I, we analyze each case and design the corresponding AP in Appendix E.

V. NUMERICAL RESULTS

In this section, we provide numerical results to demonstrate the performance of the proposed algorithm. To demonstrate the advantages of the proposed algorithm, we compare our results with the algorithm in [21] and the algorithm based on the Statistic Location Information of MUs in [18], [19], [20] (referred to SLI algorithm hereafter). In the simulation, we adopt the system model in Section II, where the radius of the MBS coverage is $R = 0.5$ km, the radius of the C-SBS coverage is $r = 0.1$ km, and 10^5 MUs are uniformly distributed in the MBS coverage. Furthermore, we assume the power of the AWGN $\sigma^2 = -114$ dBm, the target SNR of the MU is $\gamma_{T,dB} = 20$, the IP constraint at the MU is $\eta = 0.01$, the number of blocks $I = 50$ unless otherwise specified, and the number of subblocks within each block is $J = 1$.

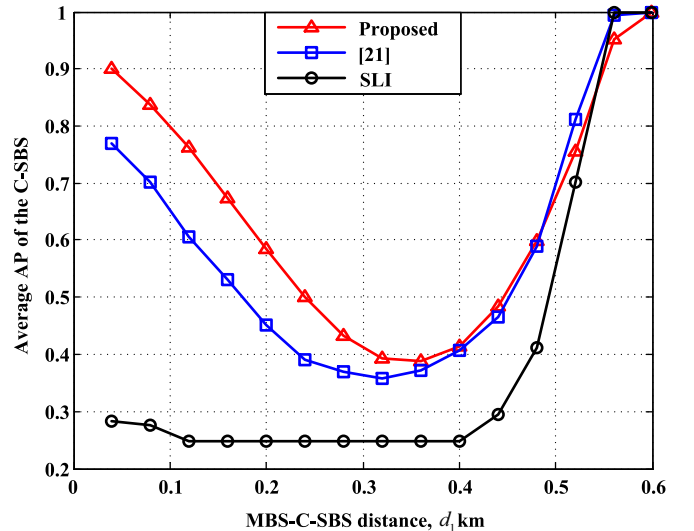


Figure 4. The comparison of the APs with different algorithms.

Fig. 4 compares the AP of the proposed algorithm with the algorithm in [21] and the SLI. From this figure, we observe that the curve of the AP with the proposed algorithm is a “U” shape. In particular, the AP of the proposed algorithm first decreases from around 0.9 to around 0.4 as the MBS-C-SBS distance d_1 grows from 0.04 km to 0.36 km, and then increases from around 0.4 to around 1 as d_1 grows from 0.36 km to 0.6 km. The reason is that, when d_1 is small, the area of the interference region increases as d_1 grows. This reduces the AP of the C-SBS. When d_1 is large, the area of the interference region reduces as d_1 grows. This increases the AP of the C-SBS. Besides, the proposed algorithm outperforms both the algorithm in [21] and the SLI, when the C-SBS is in the MBS coverage, i.e., $d_1 \leq R = 0.5$ km. Specifically, the proposed algorithm is able to improve the AP by up to 15% compared with the algorithm in [21] and improve the AP by up to 60% compared with the SLI algorithm. This figure also indicates that the C-SBS can obtain a high AP when the C-SBS is deployed close to or far away from the MBS.

Fig. 5 provides the IP of different algorithms corresponding to the AP in Fig. 4. In general, the IP with the proposed algorithm is below the IP constraint $\eta = 0.01$ except for $0.37 \leq d_1 \leq 0.5$ km, where the maximum IP is around 0.012. In fact, the accuracy of the designed AP is affected by the AWGN. With a finite number of samples K , the designed AP is not accurate. Thus, there is a chance that the IP constraint $\eta = 0.01$ at the MU is violated with the designed AP. Besides, we observe that the IP with the algorithm in [21] is above the IP constraint $\eta = 0.01$ for $0.17 \leq d_1 \leq 0.52$ km. And the IP with the SLI algorithm is above the IP constraint $\eta = 0.01$ for $0.24 \leq d_1 \leq 0.52$ km. Thus, the C-SBS with the proposed algorithm can be deployed in a wider region than the C-SBS with the algorithm in [21] and the SLI algorithm.

Fig. 6 investigates the impact of the number of blocks I on the AP of different algorithms. With the proposed algorithm, the AP increases as I grows from 50 to 100 for small d_1 , i.e., $d_1 \leq 0.36$ km, and remains constant as I grows from 50 to 100 for large d_1 , i.e., $d_1 > 0.36$ km. The reason is that, each

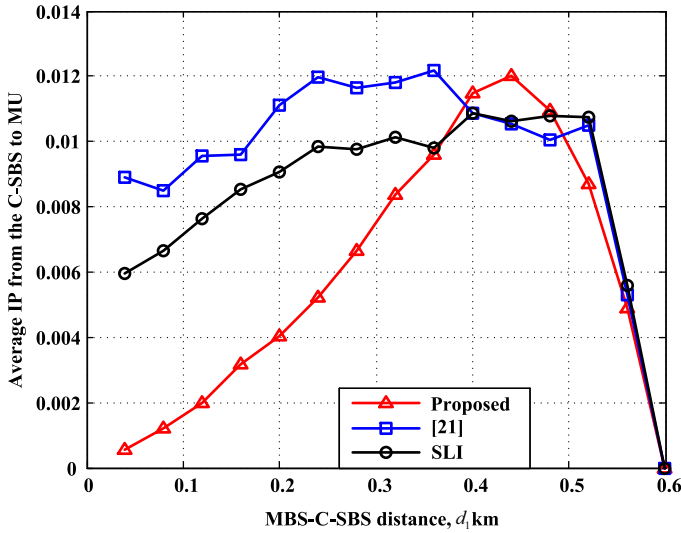


Figure 5. IP from the C-SBS to the MU with different algorithms corresponding to the AP in Fig. 4.

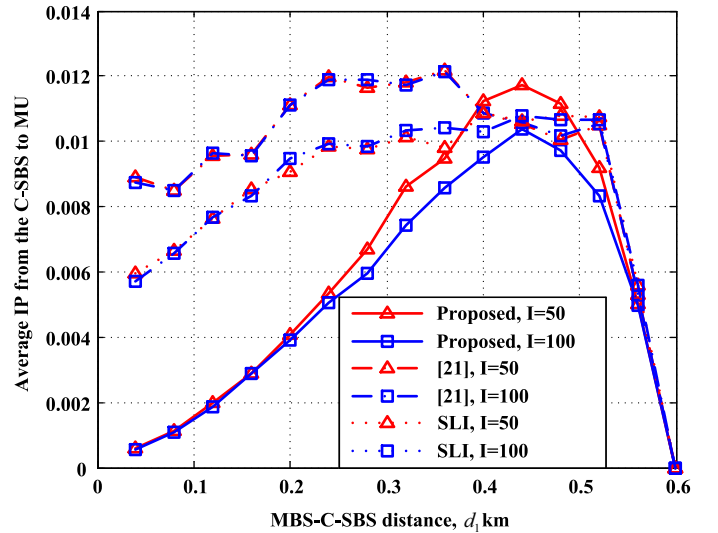


Figure 7. IP with different number of blocks I .

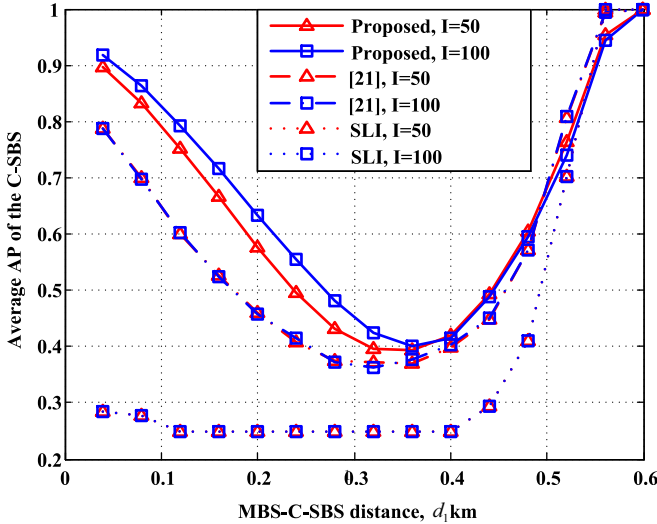


Figure 6. AP with different number of blocks I .

measured SNR at the C-SBS contains both the information of d_1 and the noise. When d_1 is small, the measured SNR is large and contains more information of d_1 than the noise. Then, the C-SBS can learn more accurate information of d_1 with more blocks, and obtain a larger AP. When d_1 is large, the measured SNR is small and contains more noise than the information of d_1 . Then, the increase of blocks has little impact on the AP. On the other hand, the AP always remains constant as I grows from 50 to 100 with the algorithm in [21] and the SLI algorithm.

Fig. 7 investigates the impact of the number of blocks I on the IP of different algorithms. With the proposed algorithm, the IP decreases as I grows. In particular, the IP is generally smaller than the IP constraint $\eta = 0.01$ when I is larger than 100. This indicates that the IP performance with the proposed algorithm can be optimized by increasing I . With the algorithm in [21], the IP always remains constant as I grows. By combining Fig. 6 and Fig. 7, we demonstrate that

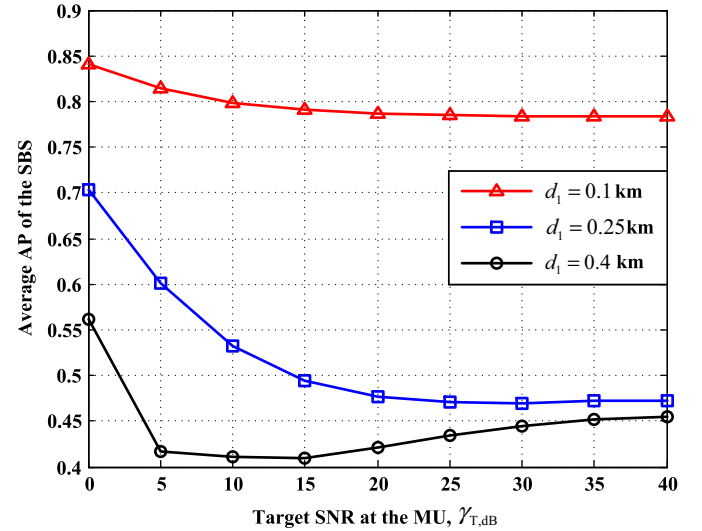


Figure 8. AP with different target SNRs at the MU in different scenarios.

the increase of I may improve the AP and reduce the IP with the proposed algorithm. However, the algorithm in [21] and the SLI algorithm are not sensitive to I . In other words, the C-SBS cannot satisfy the IP constraint by increasing I . This limits the application of the algorithm in [21] and the SLI algorithm.

Fig. 8 studies the AP with different target SNRs at MUs in different scenarios. In particular, when $d_1 = 0.1$ km, i.e., Scenario I, the AP of the C-SBS is calculated by (28) in Case I, (31) in Case II, (34) in Case III, (37) in Case IV, (40) in Case V, or (43) in Case VI. We observe that the AP of the C-SBS decreases as γ_T grows. Since the AP is related to six cases, it is difficult to analyze the trend of the AP theoretically. Instead, we study the probabilities of different cases in Fig. 9. From Fig. 9, the AP is mainly determined by Case II and Case IV. In particular, the probabilities of Case II and Case IV decrease and increase as γ_T grows, respectively. We also provide the average values of (31) in Case II and (37) in Case

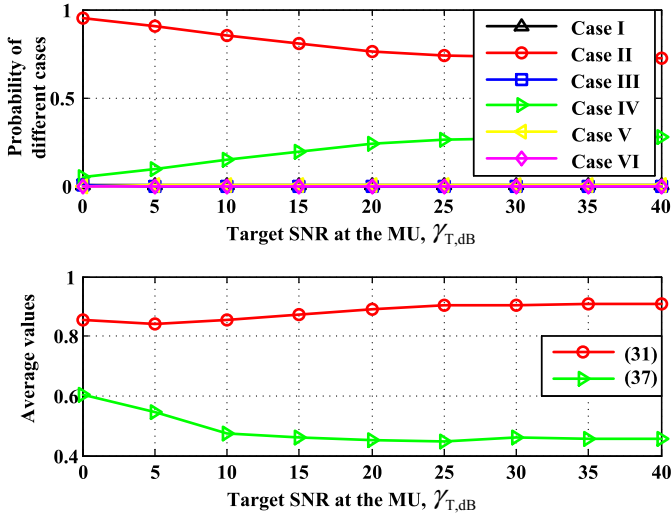


Figure 9. The upper subfigure provides the probabilities of different cases for $d_1 = 0.1$ km in the simulation; the lower subfigure provides the average values of (31) in Case II and (37) in Case IV in the simulation.

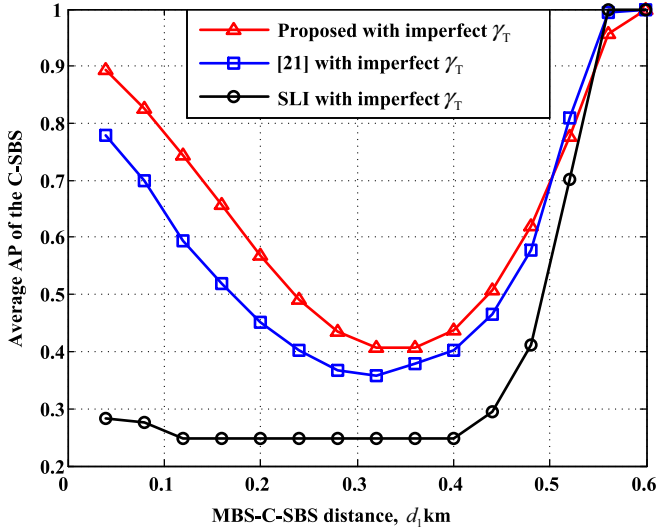


Figure 10. AP performance of different algorithms with imperfect target SNR γ_T . In particular, real $\gamma_{T,dB}$ is uniformly distributed between 17 dB and 23 dB, and the estimated target SNR $\gamma_{T,dB} = 20$ dB.

IV. Since the average value of (31) in Case II is much larger than that of (37) in Case IV, the overall decreases as γ_T grows. The AP curves for $d_1 = 0.25$ km (Scenario II) and $d_1 = 0.4$ km (Scenario III) can be similarly analyzed.

In the proposed algorithm, the target SNR $\gamma_{T,dB}$ of the MU is needed at the C-SBS to design the AP and satisfy the IP constraint at the MU. However, the information of $\gamma_{T,dB}$ is unknown at the C-SBS. Although $\gamma_{T,dB}$ can be estimated at the C-SBS by observing the *modulation and coding scheme* (MCS) of the MBS signal, there may exist some estimation errors of $\gamma_{T,dB}$. Here, we consider imperfect $\gamma_{T,dB}$ at the C-SBS and compare the performance of different algorithms. In particular, we assume that $\gamma_{T,dB}$ is uniformly distributed between 17 dB and 23 dB. In other words, the estimated target SNR $\gamma_{T,dB} = 20$ dB has up to ± 3 dB errors. The AP and IP performance is provided in Fig. 10 and Fig. 11, respectively.

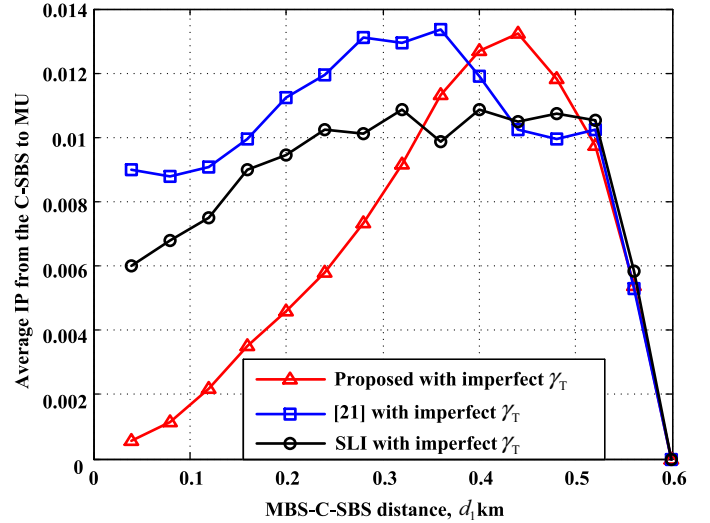


Figure 11. IP performance of different algorithms with imperfect target SNR γ_T . In particular, real $\gamma_{T,dB}$ is uniformly distributed between 17 dB and 23 dB, the estimated target SNR $\gamma_{T,dB} = 20$ dB.

By comparing the AP performance with perfect target SNR $\gamma_{T,dB}$ in Fig. 4 and the AP performance with imperfect target SNR $\gamma_{T,dB}$ in Fig. 10, imperfect target SNR $\gamma_{T,dB}$ has little impact on the AP performance. Meanwhile, by comparing the IP performance with perfect target SNR $\gamma_{T,dB}$ in Fig. 5 and the IP performance with imperfect target SNR $\gamma_{T,dB}$ in Fig. 11, imperfect target SNR $\gamma_{T,dB}$ may slightly increase the IP with the proposed algorithm and the algorithm in [21], and has little impact on the SLI algorithm (Since the SLI algorithm is independent on target SNR $\gamma_{T,dB}$). In particular, the IP with the proposed algorithm is below the IP constraint $\eta = 0.01$ except for $0.34 \leq d \leq 0.52$ km, and the IP with the algorithm in [21] is below the IP constraint $\eta = 0.01$ except for $0.34 \leq d \leq 0.52$ km, and the IP with the SLI algorithm is below the IP constraint $\eta = 0.01$ except for $0.24 \leq d \leq 0.52$ km. Thus, the proposed algorithm can be applied in a wider region compared with the algorithms in [21] and the SLI algorithm, even when the target SNR $\gamma_{T,dB}$ is imperfect.

Besides, to satisfy the IP constraint with the proposed algorithm for $0.34 \leq d \leq 0.52$ km in the practical deployment, two schemes may be adopted. The first one is to increase the number of blocks as shown in Fig. 6 (if possible). The second one is to reduce the AP for $0.34 \leq d \leq 0.52$ km. For instance, for $d_1 = 0.44$ km, the AP and IP are around 0.5 and 0.013, respectively. Then, we reduce the AP as $\rho_{AP} = 0.5 \times \frac{\eta}{0.013} \approx 0.4$ when considering imperfect target SNR $\gamma_{T,dB}$.

VI. CONCLUSIONS

In this paper, we proposed a learning-based method for the C-SBS to exploit the MBS-MU distance information and realize the coexistence between a cognitive small cell and a macro cell in a two-tier underlay HetNet. In particular, we first enabled the C-SBS to analyze the MBS signal and learn the MBS-MU distance information. Then, we calculated the upper bound of the probability that the MU is in the C-SBS coverage

and design an AP with a closed-form expression to satisfy the IP constraint at the MU. Numerical results indicated that the proposed algorithm outperforms the existing methods up to 60% AP (or transmission opportunity) improvement. With the proposed algorithms, the cognitive small cell can use the same frequency bands as the macro cell at the same time in a HetNet. This enhances the spectrum efficiency and provides a potential solution for the spectrum scarcity problem in the future wireless communications. Besides, the cognitive small cell can coexist with the macro cell without any centralized coordinator. This reduces the cost to deploy a cognitive small cell within a HetNet and is meaningful from the practical perspective. Furthermore, we demonstrate that the MBS-MU distance information is of great importance for a cognitive small cell to effectively coexist with the macro cell.

VII. APPENDIX

A. Proof of Lemma 1

To prove Lemma 1, we only need to verify $F_{\Gamma_{1,dB}}(\gamma_{T,dB} + 37.6 \log_{10}(\frac{d_0}{d_1})) = \frac{1}{2}$. From (15), we have

$$\begin{aligned} & F_{\Gamma_{1,dB}}\left(\gamma_{T,dB} + 37.6 \log_{10}\left(\frac{d_0}{d_1}\right)\right) \\ &= \Pr\left\{\gamma_{1,dB} \leq \gamma_{T,dB} + 37.6 \log_{10}\left(\frac{d_0}{d_1}\right)\right\} \\ &= \int_{-\infty}^{\infty} f_{\Theta_s}(\theta_s) F_{\Theta_r}(-\theta_s) d\theta_s \\ &= \int_{-\infty}^0 f_{\Theta_s}(\theta_s) \frac{1}{1+10^{\frac{\theta_s}{10}}} d\theta_s + \int_0^{\infty} f_{\Theta_s}(\theta_s) \frac{1}{1+10^{\frac{\theta_s}{10}}} d\theta_s \\ &= \int_0^{\infty} f_{\Theta_s}(-\theta_s) \frac{1}{1+10^{-\frac{\theta_s}{10}}} d\theta_s + \int_0^{\infty} f_{\Theta_s}(\theta_s) \frac{1}{1+10^{\frac{\theta_s}{10}}} d\theta_s. \quad (50) \end{aligned}$$

From (14), we observe that $f_{\Theta_s}(\theta_s)$ is an even function. Then, we have $f_{\Theta_s}(-\theta_s) = f_{\Theta_s}(\theta_s)$. Meanwhile, we have $\frac{1}{1+10^{-\frac{\theta_s}{10}}} = 1 - \frac{1}{1+10^{\frac{\theta_s}{10}}}$. Thus, (50) can be rewritten as

$$\begin{aligned} & F_{\Gamma_{1,dB}}\left(\gamma_{T,dB} + 37.6 \log_{10}\left(\frac{d_0}{d_1}\right)\right) \\ &= \int_0^{\infty} f_{\Theta_s}(\theta_s) \left(1 - \frac{1}{1+10^{\frac{\theta_s}{10}}}\right) d\theta_s + \int_0^{\infty} f_{\Theta_s}(\theta_s) \frac{1}{1+10^{\frac{\theta_s}{10}}} d\theta_s \\ &= \int_0^{\infty} f_{\Theta_s}(\theta_s) d\theta_s \\ &= \frac{1}{2}. \quad (51) \end{aligned}$$

Here, we complete the proof of Lemma 1.

B. Proof of Theorem 1

Based on the value of d_0^e , we discuss three cases as follows:

• *For the case $f(\bar{\gamma}_{1,dB}(1)) > d_0^e > 0$:* In this case, it is straightforward to obtain

$$1 = \Pr\{d_0 > 0\} > \Pr\{d_0 > d_0^e\} > \Pr\{d_0 > f(\bar{\gamma}_{1,dB}(1))\}. \quad (52)$$

Then, we calculate $\Pr\{d_0 > f(\bar{\gamma}_{1,dB}(1))\}$ in the following.

From the proof of Lemma 1, the probability that $\gamma_{1,dB}(k)$ ($1 \leq k \leq K$) is larger than or equal to $\gamma_{T,dB} + 37.6 \log_{10}(\frac{d_0}{d_1})$ is $\frac{1}{2}$. Then, the probability that $\bar{\gamma}_{1,dB}(1)$ is larger than $\gamma_{T,dB} + 37.6 \log_{10}(\frac{d_0}{d_1})$ is equal to the probability that K measured SNRs in $\bar{\gamma}_{1,dB}(k)$ ($1 \leq k \leq K$) are larger than $\gamma_{T,dB} + 37.6 \log_{10}(\frac{d_0}{d_1})$, i.e.,

$$\begin{aligned} & \Pr\left\{\bar{\gamma}_{1,dB}(1) > \gamma_{T,dB} + 37.6 \log_{10}\left(\frac{d_0}{d_1}\right)\right\} \\ &= \left(\Pr\left\{\bar{\gamma}_{1,dB}(k) > \gamma_{T,dB} + 37.6 \log_{10}\left(\frac{d_0}{d_1}\right)\right\}\right)^K \\ &= \left(\frac{1}{2}\right)^K, \quad (53) \end{aligned}$$

which can be rewritten as

$$\Pr\{d_0 < f(\bar{\gamma}_{1,dB}(1))\} = \left(\frac{1}{2}\right)^K. \quad (54)$$

Thus, we have

$$\Pr\{d_0 \geq f(\bar{\gamma}_{1,dB}(1))\} = 1 - \left(\frac{1}{2}\right)^K. \quad (55)$$

By combining (52) and (54), we have (16).

• *For the case $R > d_0^e \geq f(\bar{\gamma}_{1,dB}(K))$:* In this case, it is straightforward to obtain

$$0 = \Pr\{R \leq d_0\} < \Pr\{d_0^e \leq d_0\} \leq \Pr\{f(\bar{\gamma}_{1,dB}(K)) \leq d_0\}. \quad (56)$$

We note that the probability that $\gamma_{1,dB}(K)$ is no larger than $\gamma_{T,dB} + 37.6 \log_{10}(\frac{d_0}{d_1})$ is equal to the probability that K measured SNRs in $\bar{\gamma}_{1,dB}(k)$ ($1 \leq k \leq K$) are no larger than $\gamma_{T,dB} + 37.6 \log_{10}(\frac{d_0}{d_1})$, i.e.,

$$\begin{aligned} & \Pr\left\{\bar{\gamma}_{1,dB}(K) \leq \gamma_{T,dB} + 37.6 \log_{10}\left(\frac{d_0}{d_1}\right)\right\} \\ &= \left(\Pr\left\{\bar{\gamma}_{1,dB}(k) \leq \gamma_{T,dB} + 37.6 \log_{10}\left(\frac{d_0}{d_1}\right)\right\}\right)^K \\ &= \left(\frac{1}{2}\right)^K, \quad (57) \end{aligned}$$

which can be rewritten as

$$\Pr\{f(\bar{\gamma}_{1,dB}(K)) \leq d_0\} = \left(\frac{1}{2}\right)^K. \quad (58)$$

By combining (56) and (58), we have (17).

• *For $f(\bar{\gamma}_{1,dB}(k')) \leq d_0^e < f(\bar{\gamma}_{1,dB}(k' + 1))$, where $1 \leq k' \leq K - 1$:* In this case, it is straightforward to obtain

$$\begin{aligned} & \Pr\{f(\bar{\gamma}_{1,dB}(k' + 1)) \leq d_0\} < \Pr\{d_0^e \leq d_0\} \\ & \leq \Pr\{f(\bar{\gamma}_{1,dB}(k')) \leq d_0\}. \quad (59) \end{aligned}$$

We note that the probability that $\bar{\gamma}_{1,dB}(k')$ is no larger than $\gamma_{T,dB} + 37.6 \log_{10}(\frac{d_0}{d_1})$ is equal to the probability that at least k' out of K measured SNRs in $\gamma_{1,dB}(k)$ ($1 \leq k \leq K$) are no

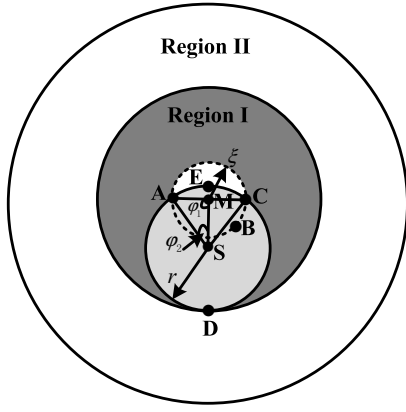


Figure 12. Geometrical model to calculate S_c in Scenario I, i.e., $\xi \leq d_1 \leq r + \xi$.

larger than $\gamma_{T,dB} + 37.6 \log_{10} \left(\frac{d_0}{d_1} \right)$, i.e.,

$$\begin{aligned} & \Pr \left\{ \bar{\gamma}_{1,dB}(k') \leq \gamma_{T,dB} + 37.6 \log_{10} \left(\frac{d_0}{d_1} \right) \right\} \\ &= C_K^{k'} \left(\frac{1}{2} \right)^{k'} \left(\frac{1}{2} \right)^{K-k'} + C_K^{k'+1} \left(\frac{1}{2} \right)^{k'+1} \left(\frac{1}{2} \right)^{K-k'-1} \\ & \quad + \dots + C_K^K \left(\frac{1}{2} \right)^K \\ &= \left(\frac{1}{2} \right)^K \left(C_K^{k'} + C_K^{k'+1} + \dots + C_K^K \right). \end{aligned} \quad (60)$$

Then, we have

$$\begin{aligned} & \Pr \left\{ d_1 10^{\frac{\bar{\gamma}_{1,dB}(k') - \gamma_{T,dB}}{37.6}} \leq d_0 \right\} \\ &= \left(\frac{1}{2} \right)^K \left(C_K^{k'} + C_K^{k'+1} + \dots + C_K^K \right). \end{aligned} \quad (61)$$

Similarly, we have

$$\begin{aligned} & \Pr \left\{ d_1 10^{\frac{\bar{\gamma}_{1,dB}(k'+1) - \gamma_{T,dB}}{37.6}} \leq d_0 \right\} \\ &= \left(\frac{1}{2} \right)^K \left(C_K^{k'+1} + C_K^{k'+2} + \dots + C_K^K \right). \end{aligned} \quad (62)$$

Combining (59), (61), and (62), we have (18). Here, we complete the proof of this theorem.

C. Derivation of S_c in Scenario I

In this part, we consider that the MU is in Scenario I and calculate the area S_c . Without loss of generality, we show the geometrical model in Fig. 12. In the sequential, we denote $o(\iota)$ as the circle region centered by point “o” with radius ι .

When $\xi \leq d_1 \leq r - \xi$, $M(\xi)$ is in the $S(r)$. Then, we have

$$S_c = \pi r^2 - \pi \xi^2. \quad (63)$$

When $r - \xi < d_1 \leq r + \xi$, $M(\xi)$ intersects with $S(r)$. We first draw auxiliary segments MA, MC, SA, SC, and MS. Then, we have $MA=MC=\xi$, $SA=SC=r$, and $MS=d_1$. Then, we denote “B” as a point both on the edge of $M(\xi)$ and in $S(r)$, denote “D” as a point on the edge of both $S(r)$ and $M(d_1+r)$, and denote “E” as a point both on the edge of $S(r)$ and in

$M(\xi)$. Besides, we denote $\angle AMS = \varphi_1$ and $\angle ASM = \varphi_2$. According to the cosine theorem, we have

$$r^2 = \xi^2 + d_1^2 - 2\xi d_1 \cos \varphi_1 \quad (64)$$

and

$$\xi^2 = r^2 + d_1^2 - 2rd_1 \cos \varphi_2. \quad (65)$$

Thus, we obtain φ_1 and φ_2 as

$$\varphi_1 = \arccos \frac{\xi^2 + d_1^2 - r^2}{2\xi d_1} \quad (66)$$

and

$$\varphi_2 = \arccos \frac{r^2 + d_1^2 - \xi^2}{2rd_1}. \quad (67)$$

Then, we have

$$\begin{aligned} S_c &= S_{ABCD} \\ &= \pi r^2 - S_{ABCE} \\ &= \pi r^2 - (S_{ABCM} + S_{ASCE} - S_{ASCM}) \\ &= \pi r^2 - \varphi_1 \xi^2 - \varphi_2 r^2 + \xi d_1 \sin \varphi_1 \\ &= (\pi - \varphi_2) r^2 - \varphi_1 \xi^2 + \xi d_1 \sin \varphi_1. \end{aligned} \quad (68)$$

By combining (63) and (68), we obtain (25).

D. AP design in Scenario II

In this part, we analyze each case in Scenario II separately. In particular, we first calculate the probability ρ_{II} that the MU is in Region II for each case and then design the corresponding AP. In the sequential, we denote $S_{II} = \pi(d_1+r)^2 - \pi(d_1-r)^2$ as the area of Region II and denote $S_c = \pi r^2$ as the area of the interference region, where the MU may appear in the C-SBS coverage.

1) *AP Design in Case I:* In this case, $d_1 - r$ satisfies (44) and $d_1 + r$ satisfies (22). The probability ρ_{II} that the MU is in Region II is

$$\begin{aligned} \rho_{II} &= \Pr \{ d_1 - r \leq d_0 \leq d_1 + r \} \\ &= \Pr \{ d_0 > d_1 - r \} - \Pr \{ d_0 > d_1 + r \} \\ &\stackrel{(II-a)}{\leq} 1 - 1 + \left(\frac{1}{2} \right)^K \\ &= \left(\frac{1}{2} \right)^K, \end{aligned} \quad (69)$$

where we use (16) in (II-a).

To control the IP constraint η at the MU, the AP of the C-SBS needs to satisfy $0 \leq \rho_{AP} \leq 1$ and $\rho_{AP} \rho_{II} \frac{S_c}{S_{II}} \leq \eta$, i.e., $\rho_{AP} \leq \min \left\{ \frac{\eta S_{II}}{\rho_{II} S_c}, 1 \right\} = \min \left\{ \frac{\eta [(d_1+r)^2 - (d_1-r)^2]}{\rho_{II} r^2}, 1 \right\}$, which can be lower bounded by

$$\begin{aligned} & \min \left\{ \frac{\eta [(d_1+r)^2 - (d_1-r)^2]}{\rho_{II} r^2}, 1 \right\} \\ &\stackrel{(II-b)}{\geq} \min \left\{ \frac{\eta 2^K [(d_1+r)^2 - (d_1-r)^2]}{r^2}, 1 \right\}, \end{aligned} \quad (70)$$

where we use (69) in (II-b).

Thus, to protect the MU in this case, the maximum AP of

the C-SBS is

$$\rho_{\text{AP}} = \min \left\{ \frac{\eta 2^K [(d_1 + r)^2 - (d_1 - r)^2]}{r^2}, 1 \right\}. \quad (71)$$

2) *AP Design in Case II:* In this case, $d_1 - r$ satisfies (44) and $d_1 + r$ satisfies (23). The probability ρ_{II} that the MU is in Region II is

$$\begin{aligned} \rho_{\text{II}} &= \Pr \{d_0 > d_1 - r\} - \Pr \{d_0 > d_1 + r\} \\ &\stackrel{\text{(II-c)}}{\leq} 1 - \left(\frac{1}{2}\right)^K (C_K^{k_2+1} + C_K^{k_2+2} + \dots + C_K^K) \\ &= \left(\frac{1}{2}\right)^K (C_K^0 + C_K^1 + \dots + C_K^{k_2}), \end{aligned} \quad (72)$$

where we use (16) and (18) in (II-c).

To control the IP constraint η at the MU, the AP of the C-SBS needs to satisfy $0 \leq \rho_{\text{AP}} \leq 1$ and $\rho_{\text{AP}} \rho_{\text{II}} \frac{S_c}{S_{\text{II}}} \leq \eta$, i.e.,

$$\rho_{\text{AP}} \leq \min \left\{ \frac{\eta S_{\text{II}}}{\rho_{\text{II}} S_c}, 1 \right\} = \min \left\{ \frac{\eta [(d_1 + r)^2 - (d_1 - r)^2]}{\rho_{\text{II}} r^2}, 1 \right\}, \text{ which can be lower bounded by}$$

$$\begin{aligned} &\min \left\{ \frac{\eta [(d_1 + r)^2 - (d_1 - r)^2]}{\rho_{\text{II}} r^2}, 1 \right\} \\ &\stackrel{\text{(II-d)}}{\geq} \left\{ \frac{\eta 2^K [(d_1 + r)^2 - (d_1 - r)^2]}{(C_K^0 + C_K^1 + \dots + C_K^{k_2}) r^2}, 1 \right\}, \end{aligned} \quad (73)$$

where we use (72) in (II-d).

Thus, to protect the MU in this case, the maximum AP of the C-SBS is

$$\rho_{\text{AP}} = \left\{ \frac{\eta 2^K [(d_1 + r)^2 - (d_1 - r)^2]}{(C_K^0 + C_K^1 + \dots + C_K^{k_2}) r^2}, 1 \right\}. \quad (74)$$

3) *AP Design in Case III:* In this case, $d_1 - r$ satisfies (44) and $d_1 + r$ satisfies (24). The probability ρ_{II} that the MU is in Region II is

$$\rho_{\text{II}} = \Pr \{d_0 > d_1 - r\} - \Pr \{d_0 > d_1 + r\} \stackrel{\text{(II-e)}}{\leq} 1, \quad (75)$$

where we use (16) and (17) in (II-e).

To control the IP constraint η at the MU, the AP of the C-SBS needs to satisfy $0 \leq \rho_{\text{AP}} \leq 1$ and $\rho_{\text{AP}} \rho_{\text{II}} \frac{S_c}{S_{\text{II}}} \leq \eta$, i.e.,

$$\rho_{\text{AP}} \leq \min \left\{ \frac{\eta S_{\text{II}}}{\rho_{\text{II}} S_c}, 1 \right\} = \min \left\{ \frac{\eta [(d_1 + r)^2 - (d_1 - r)^2]}{\rho_{\text{II}} r^2}, 1 \right\}, \text{ which can be lower bounded by}$$

$$\begin{aligned} &\min \left\{ \frac{\eta [(d_1 + r)^2 - (d_1 - r)^2]}{\rho_{\text{II}} r^2}, 1 \right\} \\ &\stackrel{\text{(II-f)}}{\geq} \min \left\{ \frac{\eta [(d_1 + r)^2 - (d_1 - r)^2]}{r^2}, 1 \right\}, \end{aligned} \quad (76)$$

where we use (75) in (II-f).

Thus, to protect the MU in this case, the maximum AP of the C-SBS is

$$\rho_{\text{AP}} = \min \left\{ \frac{\eta [(d_1 + r)^2 - (d_1 - r)^2]}{r^2}, 1 \right\}. \quad (77)$$

4) *AP Design in Case IV:* In this case, $d_1 - r$ satisfies (45) and $d_1 + r$ satisfies (23). The probability ρ_{II} that the MU is

in Region II is

$$\begin{aligned} \rho_{\text{II}} &= \Pr \{d_0 > d_1 - r\} - \Pr \{d_0 > d_1 + r\} \\ &\stackrel{\text{(II-g)}}{\leq} \left(\frac{1}{2}\right)^K (C_K^{k_1} + C_K^{k_1+1} + \dots + C_K^K) \\ &\quad - \left(\frac{1}{2}\right)^K (C_K^{k_2+1} + C_K^{k_2+2} + \dots + C_K^K) \\ &= \left(\frac{1}{2}\right)^K (C_K^{k_1} + C_K^{k_1+1} + \dots + C_K^{k_2}), \end{aligned} \quad (78)$$

where we use (18) in (II-g).

To control the IP constraint η at the MU, the AP of the C-SBS needs to satisfy $0 \leq \rho_{\text{AP}} \leq 1$ and $\rho_{\text{AP}} \rho_{\text{II}} \frac{S_c}{S_{\text{II}}} \leq \eta$, i.e.,

$$\rho_{\text{AP}} \leq \min \left\{ \frac{\eta S_{\text{II}}}{\rho_{\text{II}} S_c}, 1 \right\} = \min \left\{ \frac{\eta [(d_1 + r)^2 - (d_1 - r)^2]}{\rho_{\text{II}} r^2}, 1 \right\}, \text{ which can be lower bounded by}$$

$$\begin{aligned} &\min \left\{ \frac{\eta [(d_1 + r)^2 - (d_1 - r)^2]}{\rho_{\text{II}} r^2}, 1 \right\} \\ &\stackrel{\text{(II-h)}}{\geq} \min \left\{ \frac{\eta 2^K [(d_1 + r)^2 - (d_1 - r)^2]}{r^2 (C_K^{k_1} + C_K^{k_1+1} + \dots + C_K^{k_2})}, 1 \right\}, \end{aligned} \quad (79)$$

where we use (78) in (II-h).

Thus, to protect the MU in this case, the maximum AP of the C-SBS is

$$\rho_{\text{AP}} = \min \left\{ \frac{\eta 2^K [(d_1 + r)^2 - (d_1 - r)^2]}{r^2 (C_K^{k_1} + C_K^{k_1+1} + \dots + C_K^{k_2})}, 1 \right\}. \quad (80)$$

5) *AP Design in Case V:* In this case, $d_1 - r$ satisfies (45) and $d_1 + r$ satisfies (24). The probability ρ_{II} that the MU is in Region II is

$$\begin{aligned} \rho_{\text{II}} &= \Pr \{d_0 > d_1 - r\} - \Pr \{d_0 > d_1 + r\} \\ &\stackrel{\text{(II-i)}}{\leq} \left(\frac{1}{2}\right)^K (C_K^{k_1} + C_K^{k_1+1} + \dots + C_K^K), \end{aligned} \quad (81)$$

where we use (17) and (18) in (II-i).

To control the IP constraint η at the MU, the AP of the C-SBS needs to satisfy $0 \leq \rho_{\text{AP}} \leq 1$ and $\rho_{\text{AP}} \rho_{\text{II}} \frac{S_c}{S_{\text{II}}} \leq \eta$, i.e.,

$$\rho_{\text{AP}} \leq \min \left\{ \frac{\eta S_{\text{II}}}{\rho_{\text{II}} S_c}, 1 \right\} = \min \left\{ \frac{\eta [(d_1 + r)^2 - (d_1 - r)^2]}{\rho_{\text{II}} r^2}, 1 \right\}, \text{ which can be lower bounded by}$$

$$\begin{aligned} &\min \left\{ \frac{\eta [(d_1 + r)^2 - (d_1 - r)^2]}{\rho_{\text{II}} r^2}, 1 \right\} \\ &\stackrel{\text{(II-j)}}{\geq} \min \left\{ \frac{\eta 2^K [(d_1 + r)^2 - (d_1 - r)^2]}{r^2 (C_K^{k_1} + C_K^{k_1+1} + \dots + C_K^K)}, 1 \right\}, \end{aligned} \quad (82)$$

where we use (81) in (II-j).

Thus, to protect the MU in this case, the maximum AP of the C-SBS is

$$\rho_{\text{AP}} = \min \left\{ \frac{\eta 2^K [(d_1 + r)^2 - (d_1 - r)^2]}{r^2 (C_K^{k_1} + C_K^{k_1+1} + \dots + C_K^K)}, 1 \right\}. \quad (83)$$

6) *AP Design in Case VI:* In this case, $d_1 - r$ satisfies (46) and $d_1 + r$ satisfies (24). The probability ρ_{II} that the MU is

in Region II is

$$\rho_{\text{II}} = \Pr\{d_0 > d_1 - r\} - \Pr\{d_0 > d_1 + r\} \stackrel{\text{(II-k)}}{\leq} \left(\frac{1}{2}\right)^K, \quad (84)$$

where we use (17) in (II-k).

To control the IP constraint η at the MU, the AP of the C-SBS needs to satisfy $0 \leq \rho_{\text{AP}} \leq 1$ and $\rho_{\text{AP}}\rho_{\text{II}}\frac{S_c}{S_{\text{II}}} \leq \eta$, i.e., $\rho_{\text{AP}} \leq \min\left\{\frac{\eta S_{\text{II}}}{\rho_{\text{II}} S_c}, 1\right\} = \min\left\{\frac{\eta[(d_1+r)^2 - (d_1-r)^2]}{\rho_{\text{II}} r^2}, 1\right\}$, which can be lower bounded by

$$\begin{aligned} & \min\left\{\frac{\eta[(d_1+r)^2 - (d_1-r)^2]}{\rho_{\text{II}} r^2}, 1\right\} \\ \stackrel{\text{(II-l)}}{\geq} & \min\left\{\frac{\eta 2^K [(d_1+r)^2 - (d_1-r)^2]}{r^2}, 1\right\}, \end{aligned} \quad (85)$$

where we use (84) in (II-l).

Thus, to protect the MU in this case, the maximum AP of the C-SBS is

$$\rho_{\text{AP}} = \min\left\{\frac{\eta 2^K [(d_1+r)^2 - (d_1-r)^2]}{r^2}, 1\right\}. \quad (86)$$

E. AP Design in Scenario III

In this part, we analyze each case in Scenario III separately. In particular, we first calculate the probability ρ_{I} that the MU is in Region II for each case and then design the corresponding AP. In the sequential, we denote $S_{\text{II}} = \pi R^2 - \pi(d_1 - r)^2$ as the area of Region II and denote S_c as the area of the interference region, where the MU may appear in the coverage of the C-SBS. From Appendix F, we obtain

$$S_c = \varphi_3 R^2 + \varphi_4 r^2 - R d_1 \sin \varphi_3, \quad (87)$$

where $\varphi_3 = \arccos \frac{R^2 + d_1^2 - r^2}{2Rd_1}$ and $\varphi_4 = \arccos \frac{r^2 + d_1^2 - R^2}{2rd_1}$.

1) *AP Design in Case I:* In this case, $d_1 - r$ satisfies (44) and R satisfies (47). The probability ρ_{II} that the MU is in Region II is

$$\begin{aligned} \rho_{\text{II}} &= \Pr\{d_1 - r < d_0 \leq R\} \\ &= \Pr\{d_0 > d_1 - r\} - \Pr\{d_0 > R\} \\ \stackrel{\text{(III-a)}}{\leq} & 1 - 1 + \left(\frac{1}{2}\right)^K \\ &= \left(\frac{1}{2}\right)^K, \end{aligned} \quad (88)$$

where we use (16) in (III-a).

To control the IP constraint η at the MU, the AP of the C-SBS needs to satisfy $0 \leq \rho_{\text{AP}} \leq 1$ and $\rho_{\text{AP}}\rho_{\text{II}}\frac{S_c}{S_{\text{II}}} \leq \eta$, i.e., $\rho_{\text{AP}} \leq \min\left\{\frac{\eta S_{\text{II}}}{\rho_{\text{II}} S_c}, 1\right\} = \min\left\{\frac{\eta[\pi R^2 - \pi(d_1 - r)^2]}{\rho_{\text{II}} S_c}, 1\right\}$, which can be lower bounded by

$$\begin{aligned} & \min\left\{\frac{\eta[\pi R^2 - \pi(d_1 - r)^2]}{\rho_{\text{II}} S_c}, 1\right\} \\ \stackrel{\text{(III-b)}}{\geq} & \min\left\{\frac{\eta 2^K [\pi R^2 - \pi(d_1 - r)^2]}{S_c}, 1\right\}, \end{aligned} \quad (89)$$

where we use (88) in (III-b).

Thus, to protect the MU in this case, the maximum AP of the C-SBS is

$$\rho_{\text{AP}} = \min\left\{\frac{\eta 2^K [\pi R^2 - \pi(d_1 - r)^2]}{S_c}, 1\right\}, \quad (90)$$

where S_c is shown in (87).

2) *AP Design in Case II:* In this case, $d_1 - r$ satisfies (44) and R satisfies (48). The probability ρ_{II} that the MU is in Region II is

$$\begin{aligned} \rho_{\text{II}} &= \Pr\{d_0 > d_1 - r\} - \Pr\{d_0 > R\} \\ \stackrel{\text{(III-c)}}{\leq} & 1 - \left(\frac{1}{2}\right)^K (C_K^{k_3+1} + C_K^{k_3+2} + \dots + C_K^K) \\ &= \left(\frac{1}{2}\right)^K (C_K^0 + C_K^1 + \dots + C_K^{k_3}), \end{aligned} \quad (91)$$

where we use (16) and (18) in (III-c).

To control the IP constraint η at the MU, the AP of the C-SBS needs to satisfy $0 \leq \rho_{\text{AP}} \leq 1$ and $\rho_{\text{AP}}\rho_{\text{II}}\frac{S_c}{S_{\text{II}}} \leq \eta$, i.e., $\rho_{\text{AP}} \leq \min\left\{\frac{\eta S_{\text{II}}}{\rho_{\text{II}} S_c}, 1\right\} = \min\left\{\frac{\eta[\pi R^2 - \pi(d_1 - r)^2]}{\rho_{\text{II}} S_c}, 1\right\}$, which can be lower bounded by

$$\begin{aligned} & \min\left\{\frac{\eta[\pi R^2 - \pi(d_1 - r)^2]}{\rho_{\text{II}} S_c}, 1\right\} \\ \stackrel{\text{(III-d)}}{\geq} & \left\{\frac{\eta 2^K [\pi R^2 - \pi(d_1 - r)^2]}{(C_K^0 + C_K^1 + \dots + C_K^{k_3}) S_c}, 1\right\}, \end{aligned} \quad (92)$$

where we use (91) in (III-d).

Thus, to protect the MU in this case, the maximum AP of the C-SBS is

$$\rho_{\text{AP}} = \left\{\frac{\eta 2^K [\pi R^2 - \pi(d_1 - r)^2]}{(C_K^0 + C_K^1 + \dots + C_K^{k_3}) S_c}, 1\right\}, \quad (93)$$

where S_c is shown in (87).

3) *AP Design in Case III:* In this case, $d_1 - r$ satisfies (44) and R satisfies (49). The probability ρ_{II} that the MU is in Region II is

$$\rho_{\text{II}} = \Pr\{d_0 > d_1 - r\} - \Pr\{d_0 > R\} \stackrel{\text{(III-e)}}{\leq} 1, \quad (94)$$

where we use (16) and (17) in (III-e).

To control the IP constraint η at the MU, the AP of the C-SBS needs to satisfy $0 \leq \rho_{\text{AP}} \leq 1$ and $\rho_{\text{AP}}\rho_{\text{II}}\frac{S_c}{S_{\text{II}}} \leq \eta$, i.e., $\rho_{\text{AP}} \leq \min\left\{\frac{\eta S_{\text{II}}}{\rho_{\text{II}} S_c}, 1\right\} = \min\left\{\frac{\eta[\pi R^2 - \pi(d_1 - r)^2]}{\rho_{\text{II}} S_c}, 1\right\}$, which can be lower bounded by

$$\begin{aligned} & \min\left\{\frac{\eta[\pi R^2 - \pi(d_1 - r)^2]}{\rho_{\text{II}} S_c}, 1\right\} \\ \stackrel{\text{(III-f)}}{\geq} & \min\left\{\frac{\eta[\pi R^2 - \pi(d_1 - r)^2]}{S_c}, 1\right\}, \end{aligned} \quad (95)$$

where we use (32) in (III-f).

Thus, to protect the MU in this case, the maximum AP of

denote “E” as the intersection between $S(r)$ and $M(d_1 - r)$. Besides, we denote $\angle AMS = \varphi_3$ and $\angle ASM = \varphi_4$. According to the cosine theorem, we have

$$r^2 = R^2 + d_1^2 - 2Rd_1 \cos \varphi_3 \quad (106)$$

and

$$R^2 = r^2 + d_1^2 - 2rd_1 \cos \varphi_4. \quad (107)$$

Thus, we obtain φ_3 and φ_4 as

$$\varphi_3 = \arccos \frac{R^2 + d_1^2 - r^2}{2Rd_1} \quad (108)$$

and

$$\varphi_4 = \arccos \frac{r^2 + d_1^2 - R^2}{2rd_1}. \quad (109)$$

Then, we have

$$S_c = S_{ABCE} = S_{ABCM} + S_{ASCE} - S_{ASCM}, \quad (110)$$

where $S_{ABCM} = \varphi_3 R^2$, $S_{ASCE} = \varphi_4 r^2$, and $S_{ASCM} = Rd_1 \sin \varphi_3$.

Thus, we calculate S_c in this scenario as (87).

REFERENCES

- [1] J. G. Andrews et al., “What will 5G be?” *IEEE J. Sel. Areas Commun.*, vol. 32, no. 6, pp. 1065-1082, Jun. 2014.
- [2] L. Zhang, M. Xiao, G. Wu, and S. Li, “Efficient Scheduling and Power Allocation for D2D-Assisted Wireless Caching Networks” *IEEE Trans. Commun.*, vol. 64, no. 6, pp. 2438-2452, Jun. 2016.
- [3] J. G. Andrews, “Seven ways that HetNets are a cellular paradigm shift,” *IEEE Commun. Mag.*, vol. 51, no. 3, pp. 136-144, Mar. 2013.
- [4] J. G. Andrews, H. Claussen, M. Dohler, S. Rangan, and M. C. Reed, “Femtocells: Past, present, future,” *IEEE J. Sel. Areas Commun.*, vol. 30, no. 3, pp. 497-508, Apr. 2012.
- [5] A. Ghosh et al., “Heterogeneous cellular networks: From theory to practice,” *IEEE Commun. Mag.*, vol. 50, no. 6, pp. 54-64, Jun. 2012.
- [6] D. Liu, L. Wang, Y. Chen, M. Elkashlan, K. Wong, R. Schober, and L. Hanzo, “User Association in 5G Networks: A Survey and an Outlook,” *IEEE Commun. Surveys & Tutorials*, vol. 18, no. 2, pp. 1018-1044, Second quarter, 2016.
- [7] M. Peng, C. Wang, J. Li, H. Xiang, and V. Lau, “Recent Advances in Underlay Heterogeneous Networks: Interference Control, Resource Allocation, and Self-Organization,” *IEEE Commun. Surveys & Tutorials*, vol. 17, no. 2, pp. 700-729, Second quarter, 2015.
- [8] H. ElSawy, E. Hossain, and M. Haenggi, “Stochastic Geometry for Modeling, Analysis, and Design of Multi-Tier and Cognitive Cellular Wireless Networks: A Survey,” *IEEE Commun. Surveys & Tutorials*, vol. 15, no. 3, pp. 996-1019, Third Quarter, 2013.
- [9] Q. Zhao and B. M. Sadler, “A survey of dynamic spectrum access: Signal processing, networking, and regulatory policy,” *IEEE Signal Processing Mag.*, vol. 4, no. 3, pp. 79-89, May 2007.
- [10] A. Ghasemi and E. S. Sousa, “Fundamental limits of spectrum sharing in fading environments,” *IEEE Trans. Wireless Commun.*, vol. 6, no. 2, pp. 649-658, Feb. 2007.
- [11] T. W. Ban, W. Choi, B. C. Jung, and D. K. Sung, “Multi-user diversity in a spectrum sharing system,” *IEEE Trans. Wireless Commun.*, vol. 8, no. 1, pp. 102-106, Jan. 2009.
- [12] M. Wildemeersch et al., “Successive interference cancellation in heterogeneous cellular networks,” *IEEE Trans. Commun.*, vol. 62, no. 12, pp. 4440-4453, Dec. 2014.
- [13] R. Madan et al., “Cell association and interference coordination in heterogeneous LTE-A cellular networks,” *IEEE J. Sel. Areas Commun.*, vol. 28, no. 9, pp. 1479-1489, Dec. 2010.
- [14] D. Fooladivanda and C. Rosenberg, “Joint resource allocation and user association for heterogeneous wireless cellular networks,” *IEEE Trans. Wireless Commun.*, vol. 12, no. 1, pp. 248-257, Jan. 2013.
- [15] H. ElSawy, E. Hossain, and D. I. Kim, “HetNets with Cognitive Small Cells: User Offloading and Distributed Channel Allocation Techniques,” *IEEE Commun. Mag.*, vol. 51, no. 6, pp. 28-36, May 2013.
- [16] H. ElSawy and E. Hossain, “Two-Tier HetNets with Cognitive Femtocells: Downlink Performance Modeling and Analysis in a MultiChannel Environment,” *IEEE Trans. Mobile Computing*, vol. 13, no. 3, pp. 649-663, Mar. 2014.
- [17] L. Zhang, M. Xiao, G. Wu, G. Zhao, Y. C. Liang, and S. Li, “Energy-Efficient Cognitive Transmission With Imperfect Spectrum Sensing,” *IEEE J. Sel. Areas Commun.*, vol. 34, no. 5, pp. 1320-1335, May 2016.
- [18] J. G. Andrews, F. Baccelli, and R. K. Ganti, “A tractable approach to coverage and rate in cellular networks,” *IEEE Trans. Commun.*, vol. 59, no. 11, pp. 3122-3134, Nov. 2011.
- [19] W. Cheung, T. Q. S. Quek, and M. Kountouris, “Throughput optimization, spectrum allocation, access control in two-tier femtocell networks,” *IEEE J. Sel. Areas Commun.*, vol. 30, no. 3, pp. 561-574, Apr. 2012.
- [20] S. Mukherjee, “Distribution of downlink SINR in heterogeneous cellular networks,” *IEEE J. Sel. Areas Commun.*, vol. 30, no. 3, pp. 575-585, Apr. 2012.
- [21] L. Li, G. Zhao, and X. Zhou, “Enhancing Small Cell Transmission Opportunity Through Passive Receiver Detection in Two-Tier Heterogeneous Networks,” *IEEE Trans. Signal Processing*, vol. 63, no. 13, pp. 3461-3473, Jul. 2015.
- [22] 3GPP, *Physical Layer Aspects for Evolved Universal Terrestrial Radio Access (UTRA)*, 3GPP TR 25.814, 2006.
- [23] L. Zhang, M. Xiao, G. Wu, G. Zhao, Y.-C. Liang, and S. Li, “Proactive Cross-Channel Gain Estimation for Spectrum Sharing in Cognitive Radio,” *IEEE J. Sel. Areas Commun.*, vol. 34, no. 10, pp. 2776-2790, Oct. 2016.
- [24] R. Zhang, “On active learning and supervised transmission of spectrum sharing based cognitive radios by exploiting hidden primary radio feedback,” *IEEE Trans. Commun.*, vol. 58, no. 10, pp. 2960-2970, Oct. 2010.
- [25] H. Kim, S. Lim, H. Wang, and D. Hong, “Optimal power allocation and outage analysis for cognitive full duplex relay systems,” *IEEE Trans. Wireless Commun.*, vol. 11, no. 10, pp. 3754-3765, Oct. 2012.
- [26] D. Tse and P. Viswanath, *Fundamentals of wireless communications*. Cambridge University Press, 2005.